Fermilab

TM-991
1620.000

Eddy Currents, Dispersion Relations, and Transient Effects in Superconducting Magnets

Robert E. Shafer

9/22/80

1. Introduction

The purpose of this paper is to discuss the effects of eddy currents in superconducting magnets. Of primary interest are magnets suitable for accelerator applications, as they must operate under high ramp rate (dB/dt) conditions, but the effect is important in other applications as well. For example, eddy currents are sometimes used to control the propagation of a quench in superconducting magnets.

Eddy currents are induced whenever a changing magnetic field is imposed on or is linked by a conducting material. This may be a structural component of a magnet, or the superconducting coil itself. The very low power loss requirements of a superconducting magnet cryogenic system make the heating effects of eddy currents important, but in addition the eddy currents can effect the magnetic field quality. The field quality can be effected either by the direct effect of the eddy currents generating additional induction fields, or by creating a frequency-dependent electrical impedance which can cause the power supply to generate current transients.

The approach taken in this paper will be to discuss the effect of eddy currents in terms of the electrical impedance of the magnet as seen at its terminals. Ideally a magnet is purely reactive (inductive). But when eddy currents are present, a real component must exist as well. As there are time constants associated with these real components, the time constants must also appear in the reactive component, as required by dispersion relations. As the reactive component represents stored magnetic energy, the eddy currents therefore produce transients in the magnetic field. If the time constants are associated with the superconducting coil, they may be of many seconds duration.

In the next section the electrical impedance of a cylindrical geometry 2n pole magnet with a concentric thin conducting tube is derived. This may be considered as representative of a beam pipe or a cryogenic vessel in a superconducting magnet. By analogy, the general form of the solution may be extended to other geometries. In section 3, the equivalent circuit and its physical interpretation is discussed. In section 4 the causal nature of impedances is reviewed. In sections 5 and 6, The effects of eddy currents in magnets are discussed in the frequency and time domains. In the last section some measurements on Fermilab magnets are presented.

2. Eddy Currents in a Thin Cylindrical Shell

We consider a cos theta coil of radius b aligned along the z axis and carrying a current density J_z given by:

$$J_z = \frac{N_c I_o}{4b} \cos n\theta \sin \omega t \quad \text{amps/meter} \qquad [1]$$

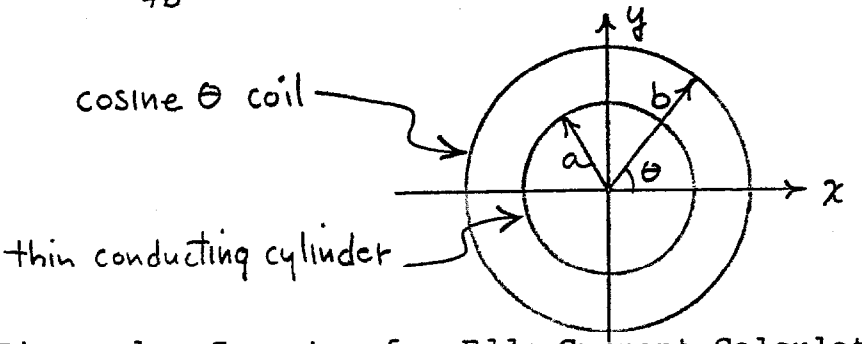

Figure 1. Geometry for Eddy Current Calculation

where N_c is the total number of conductors in the coil cross section (i.e. twice the total number of turns), and I_o is the peak excitation current in the conductors. This coil geometry generates pure multipole fields of order n in its interior. The vector potential arising from this current distribution is

$$A_z(r,\theta,t) = A_n \left(\frac{r}{b}\right)^n \cos n\theta \sin \omega t \qquad (r<b) \qquad [2]$$

$$= A_n \left(\frac{b}{r}\right)^n \cos n\theta \sin \omega t \qquad (r>b) \qquad [3]$$

where

$$A_n = \frac{\mu_o N_c I_o}{8n} ; \qquad \mu_o = 4\pi \times 10^{-7} \ H/m \qquad [4]$$

since

$$\vec{\nabla} \times (\vec{\nabla} \times \vec{A}) = - \nabla^2 A_z = + \mu_o J_z \quad \text{at} \quad r = b. \qquad [5]$$

The corresponding induction fields for $r<b$ are, since curl $\vec{A} = \vec{B}$:

$$B_r(r,\theta) = \frac{1}{r} \frac{\partial A_z}{\partial \theta} = \frac{-n A_n}{b} \left(\frac{r}{b}\right)^{n-1} \sin n\theta \sin \omega t \qquad [6]$$

$$B_\theta(r,\theta) = - \frac{\partial A_z}{\partial r} = \frac{-n A_n}{b} \left(\frac{r}{b}\right)^{n-1} \cos n\theta \sin \omega t \qquad [7]$$

We now consider a thin conducting shell of radius a and area resistivity ρ_s ohms/square placed concentrically inside the co .. When this conducting shell is placed in the coil, currents J_z' are induced in it. These currents in turn generate an additional vector potential A_z' . In particular, at $r = a$:

$$\nabla^2 (A_z + A_z') = \nabla^2 A_z' = - \mu_o J_z' \qquad [8]$$

since $\nabla^2 A_z = 0$ here. In addition, neglecting displacement currents,

$$-\frac{d}{dt}(A_z + A_z') = \rho_s J_z' = A_z'/\tau_n \qquad [9]$$

where we have defined

$$\tau_n = \frac{\mu_0 a}{2n\rho_s} \qquad [10]$$

We assume a solution of the form

$$A_z' = A_n' \cos n\theta \cos(\omega t - \epsilon_n) \begin{cases} \times (r/a)^n, & r<a \\ \times (a/r)^n, & r>a \end{cases} \qquad [11]$$

and find on substitution

$$\epsilon_n = \tan^{-1}(\omega\tau_n) \qquad [12]$$

and

$$A_n' = -A_n\left(\frac{a}{b}\right)^n \sin\epsilon_n \qquad [13]$$

Hence the new vector potential, including the induced term, is:

$$A_{TOT} = \left[\left(\frac{r}{b}\right)^n \sin\omega t - \left(\frac{r}{b}\right)^n \sin\epsilon_n \cos(\omega t - \epsilon_n)\right] A_n \cos n\theta \qquad (r<a) \qquad [14]$$

$$= \left[\left(\frac{r}{b}\right)^n \sin\omega t - \left(\frac{a^2}{br}\right)^n \sin\epsilon_n \cos(\omega t - \epsilon_n)\right] A_n \cos n\theta \qquad (a<r<b) \qquad [15]$$

$$= \left[\left(\frac{b}{r}\right)^n \sin\omega t - \left(\frac{a^2}{br}\right)^n \sin\epsilon_n \cos(\omega t - \epsilon_n)\right] A_n \cos n\theta \qquad (r>b) \qquad [16]$$

For $r<a$ the vector potential may be written

$$A_{TOT} = A_n\left(\frac{r}{b}\right)^n \cos\epsilon_n \sin(\omega t - \epsilon_n) \cos n\theta \qquad [17]$$

showing that the potential inside the conducting shell is retarded by a time $\epsilon_n/\omega \sim \tau_n$ and attenuated by a factor $\cos\epsilon_n$ relative to the case without the conducting shell.

We now want to calculate the induced voltage at the coil terminals as a function of ω. If the length of the coil in the z direction is ℓ, then the voltage induced in a single conductor at a location b, θ is:

$$-\frac{d}{dt} A_{TOT}\Big|_{r=b} \cdot \ell = \ell A_n \frac{d}{dt}\left[\left(\frac{a}{b}\right)^{2n} \sin\epsilon_n \cos(\omega t - \epsilon_n) - \sin\omega t\right] \cos n\theta \qquad [18]$$

Since the conductor density is $\frac{N_c}{4b}\cos n\theta$, the total induced voltage at the coil terminals is

$$V(\omega) = \frac{\ell A_n N_c}{4b} \frac{d}{dt}\left[\left(\frac{a}{b}\right)^{2n} \sin\epsilon_n \cos(\omega t - \epsilon_n) - \sin\omega t\right] \int_0^{2\pi} b \cos^2 n\theta \, d\theta \qquad [19]$$

Therefore

$$V(\omega) = -\frac{\mu_0 N_c^2 \ell \pi}{32n}\left\{\omega \sin\epsilon_n \cos\epsilon_n \left(\frac{a}{b}\right)^{2n} + \left[1 - \sin^2\epsilon_n \left(\frac{a}{b}\right)^{2n}\right]\frac{d}{dt}\right\} I(\omega) \qquad [20]$$

where

$$I(\omega) = I_0 \sin\omega t \qquad [21]$$

Hence we may write the coil impedance as:

$$Z(\omega) = \frac{-V(\omega)}{I(\omega)} = \frac{\mu_0 N_c^2 \ell \pi}{32n}\left\{\omega \sin\epsilon_n \cos\epsilon_n \left(\frac{a}{b}\right)^{2n} + \left[1 - \sin^2\epsilon_n \left(\frac{a}{b}\right)^{2n}\right] s\right\} \qquad [22]$$

where the Laplace operator s is given by:

$$s = \frac{d}{dt} \qquad [23]$$

3. Equivalent Circuit for Eddy Currents

The impedance in eqn [22] may be written ($L(\omega)$ and $R(\omega)$ are AC, i.e. frequency dependent, values):

$$Z(\omega) = R(\omega) + L(\omega)s = R(\omega) + j\omega L(\omega) \qquad [24]$$

where

$$L(\omega) = (1-k)L + \frac{kL}{1+(\omega\tau_n)^2} \qquad [25]$$

and

$$R(\omega) = \frac{(\omega\tau_n)^2 R}{1+(\omega\tau_n)^2} \qquad [26]$$

This impedance is represented by the equivalent circuit in Figure 2 (k, L, and R are fixed DC values):

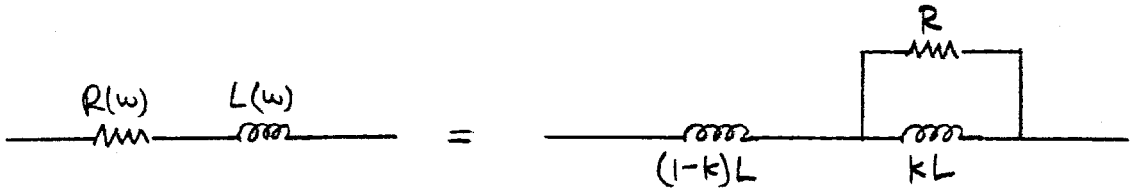

Figure 2. Equivalent Circuit for Eddy Currents

where the constants used are:

$$L = \frac{\mu_0 N^2 \ell \pi}{8n} \; ; \qquad \mu_0 = 4\pi\times10^{-7}\ H/m \qquad [27]$$

$$k = (a/b)^{2n},\ a<b \; ; \quad k = (b/a)^{2n},\ b<a \qquad [28]$$

$$\tau_n = \frac{\mu_0 a}{2n\rho_s} \qquad [29]$$

$$R = kL/\tau_n \qquad [30]$$

and where N is the total number of turns in the coil, ℓ is the length, n is the harmonic number, ρ_s is the area resistivity of the conducting shell, and b and a are the radii of the coil and the conducting shell respectively.

The AC inductance $L(\omega)$ decreases from the DC value L to a value $(1-k)L$ at high frequencies. As inductance is expressable as the volume integral of magnetic energy density at unit current, the missing inductance kL at high frequencies may be interpreted as the exclusion of part of the magnetic volume from storing energy. Specifically, the inductance of the volume inside the conducting shell is $kL/2$. Hence at high frequencies the total volume of the magnet capable of storing energy is reduced by twice the magnetic volume inside the conducting shell. The coupling constant k represents the ratio of the magnetic volumes inside the conducting shell and inside the coil. For n=1 (dipole), this is just the geometrical volume ratio. It is useful to remember that half the total stored energy in this geometry magnet is stored in the volume inside the coil.

This equivalent circuit with a simple time constant is obviously a special case. In actual magnets, many sources of eddy currents will cause a variety of time constants and coupling constants, and the above relations will become summations or integrals. Nevertheless observations show that there is often one dominant time constant present, in which case the simple model suffices.

It is interesting to note that in the above model, the parallel DC resistance R is completely specified by the DC inductance L, the coupling constant k, and the time constant τ_n, parameters which can be determined by measurements of the reactive part of the impedance in either the frequency or time domain. In fact, for any passive network, knowledge of the real (or reactive) component over the complete frequency spectrum is sufficient to determine the reactive (or real) component completely. This is a fundamental property of networks, and is discussed in the next section.

4. Dispersion Relations.

The causal relation between voltage and current in a passive network requires that the network impedance satisfy the Kramers-Kronig (dispersion) relations, first applied to absorption and dispersion in optics. Good reviews of the application of dispersion relations to network theory are presented by Bode(1) and by Guillemin(2). Although there are several ways of

expressing these relations for networks, the following two forms are perhaps best for the present application:

$$L(\omega) = \frac{2}{\pi}\int_0^\infty \frac{R(\omega') - R(\omega)}{(\omega')^2 - \omega^2}\, d\omega' \qquad [31]$$

$$R(\omega) = -\frac{2\omega^2}{\pi}\int_0^\infty \frac{L(\omega') - L(\omega)}{(\omega')^2 - \omega^2}\, d\omega' \qquad + R(0) \qquad [32]$$

The resistance integral and reactance integral theorems in network theory are direct consequences of the above relations. In essence, if either the resistance or reactance is frequency dependent, the the other is also, and their relation must satisfy the above equations.

The integral relations among other things place asymtotic limits on the frequency dependence of the real and reactive components. If the circuit involves only resistance and inductance, the AC resistance must monotonically increase with frequency, but never more than quadratically. Similarly, the AC inductance must monotonically decrease with frequency. The skin effect is a special case where the resistance and inductance scale as $\sqrt{\omega}$ and $1/\sqrt{\omega}$ respectively.

5. Magnetic Effects in the Frequency Domain.

As was pointed out in section 3, as the excitation frequency is increased, the inductance decreases due to the exclusion of magnetic field from the interior volume of the conducting shell. The amplitude and phase dependence on frequency is exactly that of the current flowing in the coupled inductance kL in Figure 2. If we assume a magnet excitation current (in the leakage inductance $(1-k)L$):

$$I(\omega) = I_0 \sin \omega t \qquad [33]$$

the current $I_2(\omega)$ flowing in the coupled inductance may be calculated from the circuit equations:

$$I_2(\omega) = \frac{1 - \tau_n s}{1 - (\tau_n s)^2}\, I(\omega) = I_0 \cos\epsilon_n \sin(\omega t - \epsilon_n) \qquad [34]$$

where ϵ_n is given in eqn [12]. Hence the magnetic field is reduced in amplitude by a factor $\cos\epsilon_n$, and retarded by a phase angle ϵ_n relative to the case without the conducting shell, as could have been calculated from the vector potential in eqn [17]. It is relevant to note the dependence on the harmonic number n. If a magnet with eddy current losses is designed to have more than one harmonic component (such as in a combined function synchrotron), or if dipole and quadrupole magnets are structurally identical and powered in series, then both the amplitude ratios and the phases of the multipoles will be frequency dependent. In synchrotron parlance, this represents a tune shift.

The power dissipation in the equivalent circuit is given by

$$P(\omega) = \frac{1}{2} I_o^2 R(\omega) = \frac{1}{2} \frac{k L \tau_n}{1+(\omega\tau_n)^2} \omega^2 I_o^2 \qquad [35]$$

hence showing a quadratic frequency dependence at low frequencies, and no frequency dependence at high frequencies. Hence an eddy current loss with a time constant long compared to the period of the excitation current would appear as a DC resistance in series with the coil.

If the induction fields are calculated for the region between the coil and the conducting shell using the vector potential in eqn [15], it will be apparent that the azimuthal component of the induction field near the shell increases with increasing frequency. There are certain points near the shell (where the radial component is zero) where the total high frequency induction field is nearly twice the low frequency value. This does not violate the requirements of the dispersion relations, however, which require that the volume integral of the magnetic energy density, rather than the magnetic energy density at every point, decrease monotonically with frequency. Hence eddy currents can cause the local induction fields to either increase or decrease, depending on the precise geometry. If eddy currents are generated in the individual conductors of the coil due to their finite size, the induction fields inside the conductor will be reduced, while the fields outside will either increase or decrease.

If the conducting shell is outside the coil, as is the case of the outer cryostat wall surrounding the coil, the vector potential inside the coil becomes (compare to eqn [14]):

$$A_{TOT} = A_n \left(\frac{r}{b}\right)^n \left[\sin\omega t - \left(\frac{b}{a'}\right)^{2n} \sin\epsilon_n' \cos(\omega t - \epsilon_n')\right] \cos n\theta \; ; \quad r<b<a' \qquad [36]$$

where ϵ_n' is the new retardation for a shell of radius a'. Because of the factor $(b/a')^{2n}$, the field in the interior is only partially extinguished at high frequencies. Other properties are similar to the case with the shell inside the coil. Note that in no case are there new harmonics generated in the central region by the eddy currents.

6. Magnetic Effects in the Time Domain

Although many effects in the time domain can be easily deduced from the frequency domain behavior, certain effects such as transient response need to be dealt with in a rigorous fashion.

Consider a voltage pulse of voltage V_o and duration t_o applied to an ideal lossless magnet of inductance L. If initially there is no current in the magnet, it will ramp linearly up to a current

$$I(t) = \frac{V_o t_o}{L} \qquad t \gg t_o \qquad [37]$$

and remain at this current indefinitely as long as the voltage at the magnet terminals is held rigorously at zero volts. However, when eddy currents are present, transients will occur both at the beginning and the end of the ramp. To calculate the transients, we need to use the Laplace transform.

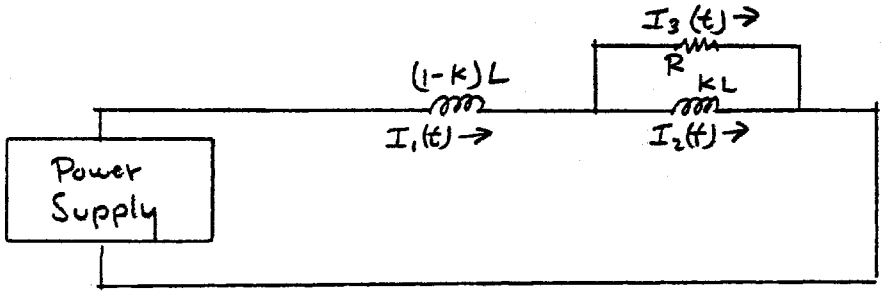

Figure 3. Equivalent Circuit for Transient Analysis

Consider the circuit in Figure 3. The circuit equations in the frequency domain are

$$V(s) = \left[(1-k)Ls + \frac{kRLs}{R+kLs}\right] I_1(s) \quad [38]$$

$$I_1(s) = I_2(s) + I_3(s) \quad [39]$$

$$R\,I_3(s) = kLs\,I_2(s) \quad [40]$$

where s is the Laplace operator. The currents in the leakage and coupled inductances are then:

$$I_1(s) = \frac{R+kLs}{RLs + (1-k)kL^2s^2}\,V(s) \quad [41]$$

$$I_2(s) = \frac{R}{RLs + (1-k)kL^2s^2}\,V(s) \quad [42]$$

where the voltage waveform described above is used:

$$V(s) = \frac{V_0}{s};\ 0 < t < t_0;\quad V(s) = 0 \quad \text{otherwise} \quad [43]$$

Using the time constants

$$\tau = \frac{kL}{R};\qquad \tau' = (1-k)\tau \quad [44]$$

the equations may be rewritten:

$$I_1(s) = \frac{V_0}{L}\left[\frac{1}{s^2(1+s\tau')} + \frac{\tau}{s(1+s\tau')}\right] \quad [45]$$

$$I_2(s) = \frac{V_0}{L}\left[\frac{1}{s^2(1+s\tau')}\right] \quad [46]$$

Carrying out the Laplace transform:

$$I_1(t) = \frac{V_0}{L}\left[t + (\tau-\tau')\left(1- e^{-t/\tau'}\right)\right] \qquad t < t_0 \qquad [47]$$

$$I_2(t) = \frac{V_0}{L}\left[t - \tau'\left(1- e^{-t/\tau'}\right)\right] \qquad t < t_0 \qquad [48]$$

which become for $t >> \tau'$

$$I_1(t) = \frac{V_0}{L}\left[t + \tau - \tau'\right] \qquad [49]$$

$$I_2(t) = \frac{V_0}{L}\left[t - \tau'\right] \qquad [50]$$

During this period, a current

$$I_3(t) = I_1(t) - I_2(t) = \frac{V_0}{L}\tau = \tau\frac{dI_1}{dt} \qquad [51]$$

is flowing in the resistance R . Hence the steady state power dissipation is:

$$P(t) = R\, I_3^2(t) = \tau^2 R\left(\frac{dI_1}{dt}\right)^2 = kL\tau\left(\frac{dI_1}{dt}\right)^2 = \alpha\left(\frac{dI_1}{dt}\right)^2 \qquad [52]$$

where, using eqn [32]:

$$\alpha = \lim_{\omega\to 0}\left[\frac{R(\omega)}{\omega^2}\right] = \frac{2}{\pi}\int_0^\infty \frac{L(0) - L(\omega')}{(\omega')^2}\,d\omega' \qquad [53]$$

The reactance integral may be integrated by parts, yielding:

$$\alpha = -\frac{2}{\pi}\int_0^\infty \frac{1}{\omega'}\,\frac{\partial L(\omega')}{\partial \omega'}\,d\omega' \qquad [54]$$

demonstrating that for $t > \tau$, the changes in inductance at low frequency are generally the major contributors to AC power losses.

After reaching a time t_0 , the applied voltage at the terminals is reduced to zero volts, and the currents become ($t > t_0$):

$$I_1(t) = \frac{V_0}{L}\left[t_0 + (\tau-\tau')\exp\left(\frac{t_0-t}{\tau'}\right)\right] \qquad [55]$$

$$I_2(t) = \frac{V_0}{L}\left[t_0 - \tau'\exp\left(\frac{t_0-t}{\tau'}\right)\right] \qquad [56]$$

Note that during the ramp the current in the coupled inductance, eqn [50], is retarded by a time τ from the applied current, eqn [49]. As already mentioned, this can produce tune shifts in strong focussing accelerators. At the end of the ramp, the applied current overshoots the final steady state value, and decays to the steady state value with the time constant τ' . The current in the coupled inductance, however, undershoots the final value, and increases to it with the same time constant.

During this process, energy in the circuit is rigorously conserved. The power supply cannot produce or absorb any energy, even when the supply current is changing, as it is set to zero volts. Some of the energy stored in the leakage inductance $(1-k)L$ is either transferred to the coupled inductance kL or dissipated in the resistance R. Any magnetic fields associated with the leakage inductance, even though they may be physically remote from the fields produced by the coupled inductance, will exhibit the overshoot transient. The basic cause is the power supply, in a voltage-controlled mode, reacting to the frequency-dependent impedance of a magnet with eddy currents.

In the case where the magnet is ramped at a constant dI/dt rather than with a constant V(t), the transients will appear in the terminal voltage of the magnet. The voltage of the circuit in Figure 3 may be written in the frequency domain for a constant dI/dt as:

$$V(s) = Z_1(s)\, I(s) = \left[(1-k)Ls + \frac{kRLs}{R+kLs}\right] \frac{1}{s^2} \frac{dI_1}{dt} \qquad [57]$$

$$= \left[\frac{(1-k)L}{s} + \frac{kL}{s(1+s\tau)}\right] \frac{dI_1}{dt} \qquad [58]$$

where

$$\tau = \frac{kL}{R} \qquad [59]$$

The Laplace transforms are:

$$V(t) = \left[(1-k)L + kL\left(1-e^{-t/\tau}\right)\right] \frac{dI_1}{dt} \qquad 0 < t < t_0 \qquad [60]$$

$$V(t) = kL \exp\left(\frac{t_0-t}{\tau}\right) \frac{dI_1}{dt} \qquad t > t_0 \qquad [61]$$

Unlike the case where the power supply was voltage controlled, the power supply continues to supply power after t_0. The current in the coupled inductance is:

$$I_2(t) = \left[t - \tau\left(1-e^{-t/\tau}\right)\right] \frac{dI_1}{dt} \qquad 0 < t < t_0 \qquad [62]$$

$$I_2(t) = \left[t_0 - \tau \exp\left(\frac{t_0-t}{\tau}\right)\right] \frac{dI_1}{dt} \qquad [63]$$

Power dissipation may again be calculated:

$$P(t) = \left[I_1(t) - I_2(t)\right]^2 R = \tau^2\left(1-e^{-t/\tau}\right)^2 R \left(\frac{dI_1}{dt}\right)^2 \approx \tau^2 R \left(\frac{dI_1}{dt}\right)^2 = \alpha \left(\frac{dI_1}{dt}\right)^2 \qquad [64]$$

The apparent inductance of the circuit may be obtained from eqn[60]:

$$L(t) = (1-k)L + kL\left(1-e^{-t/\tau}\right) \qquad [65]$$

A similar expression may be obtained by differentiating eqn [47]. In both cases the time dependent inductance increases monotonically from the minimum initial (high frequency) value to the final (DC) value. This may be considered as a statement of Lenz's law.

With regard to the possibility of transients associated with eddy currents generated in a finite thickness coil*, although skin effect type eddy currents superimposed on the transport currents will increase the current density at the inner and outer boundaries of the coil, and decrease the current density in the middle, there is no reason to expect the current densities at the two boundaries to be unequal, since the coil inductance given in eqn [27] has no dependence on the coil radius. However, if the coil is enclosed in a concentric, infinite μ, laminated iron yoke of radius c, the DC inductance becomes(3): (b = coil radius)

$$L = \frac{\mu_o N^2 \ell \pi}{8n}\left[1+\left(\frac{b}{c}\right)^{2n}\right] \quad \text{Henrys.} \qquad [66]$$

Similarly, the induction fields inside the coil, eqns [6] and [7], become: for a DC current I

$$B_r(r,\theta) = \frac{-\mu_o N I}{4b}\left[1+\left(\frac{b}{c}\right)^{2n}\right]\left(\frac{r}{b}\right)^{n-1}\sin n\theta \quad \text{tesla} \qquad [67]$$

$$B_\theta(r,\theta) = \frac{-\mu_o N I}{4b}\left[1+\left(\frac{b}{c}\right)^{2n}\right]\left(\frac{r}{b}\right)^{n-1}\cos n\theta \qquad [68]$$

and between the coil and the iron:

$$B_r(r,\theta) = \frac{-\mu_o N I}{4b}\left[1+\left(\frac{r}{c}\right)^{2n}\right]\left(\frac{b}{r}\right)^{n+1}\sin n\theta \qquad [69]$$

$$B_\theta(r,\theta) = \frac{+\mu_o N I}{4b}\left[1-\left(\frac{r}{c}\right)^{2n}\right]\left(\frac{b}{r}\right)^{n+1}\cos n\theta\,. \qquad [70]$$

Now the inductance increases as the coil radius increases. As the initial inductance is the minimum inductance, there will be a higher current density at the inner boundary of the coil than at the outside. The dependence of the inner induction fields on the coil radius is such that there will be an overshoot type transient in the central field.

The above examples should be considered as representative of wide class of eddy current losses which result in exponential transients. A transient implies the existance of an equivalent circuit of the general form shown in Figure 3, even though it is not caused by a conducting shell. The coupling constant may still be interpreted as relating to magnetic volume, but the interpretation of the time constants is more obscure. Note that in the above examples, the time constant depends on whether the power supply is a current source or a voltage source. In the latter, the leakage inductance appears to be in parallel with the

* i.e. NI amp turns of single layer rectangular cross section wire

coupled inductance. If k=.99 for example, τ' can be 100 times smaller than τ .

It is also worthwhile to note that a single conducting shell can generate more than one time constant. In the case of a conducting shell inside a dipole (n=1) coil. the shell can be displaced from the center and the time constant will remain the same. However, if the shell is displaced from the center of a quadrupole (n=2), there will be a dipole field as well as a quadrupole field imposed on the conducting shell, resulting in two time constants.

Exponential transients have been observed in magnets at Brookhaven(4). Specifically, on ramping from 0 to 1000 amps (13,400 Gauss) at 3 amps/sec., a 23 Gauss overshoot was observed in the dipole field with a 63 sec. time constant. If we assume that the magnet was powered by a voltage source, and that the central field represented part of the leakage inductance, and therefore was proportional to $I_1(t)$, such a transient can be generated in the equivalent circuit using L =120mH (design value), k =.009, and R = 17 μohms. The model also predicts an AC power loss of nearly 7 watts at a ramp rate of 10 amps/sec., approximately what was observed. The very small values of the constant k and the resistance R , the observation of an overshoot, and the very long time constant all seem to point to eddy current losses in the coil itself. Such losses have been predicted by Morgan(5). It is very likely that the observed Broookhaven transient is actually of the type discussed in connection with the iron yoke, eqn [66]. To attempt to calculate the effect quantitatively is beyond the scope of this Memo.

In another case, when an Energy Doubler correction dipole was excited with a 1Hz triangular current ramp, a τ = 80 msec, k = .04 voltage transient was observed. This was found to be associated with a closely coupled solid iron pipe just outside the coil. As this coil was wound with single strand wire rather than a braided cable, transients related to finite coil thickness were minimized.

In conclusion, there is a direct relation between the frequency dependence of inductance and the existance of transients. The existance of one predicates the existance of the other, as well as the presence of eddy current power losses.

7. Measurements on Fermilab Energy Doubler Magnets

The basic design of the Energy Doubler superconducting magnets is reviewed elsewhere(6). It is a cold bore, warm iron design with a two layer, azimuthally segmented, coil design. The coil is mechanically supported by a laminated stainless steel collar assembly. Inside the coil is a thin stainless steel bore tube about 71 mm diameter and 1.7 mm thick. Outside the collared coil

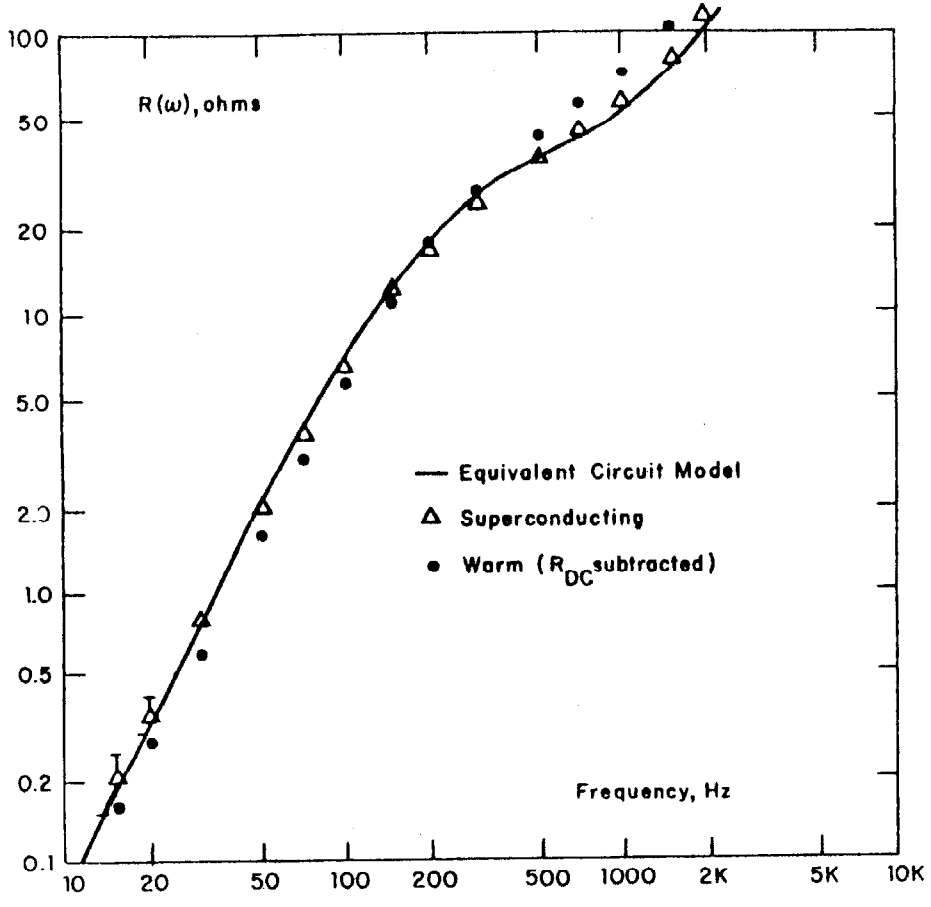

Figure 4. Resistive component of Energy Doubler magnet impedance vs. frequency

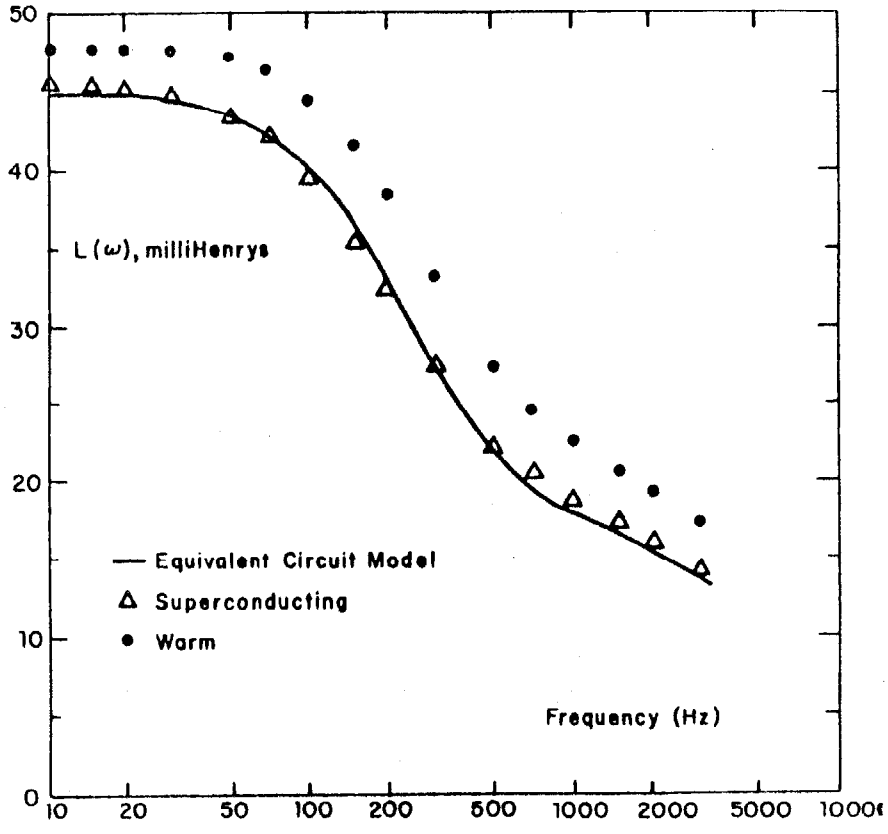

Figure 5. Inductive component of Energy Doubler magnet impedance vs. frequency

assembly is the cryogenic system, consisting of five concentric stainless steel tubes, average diameter about 163 mm, total thickness about 5.9 mm. Outside the cryogenic system is a laminated iron yoke. The bore tube is very closely coupled to the coil, while the coil to cryostat diameter ratio is about 0.6. This implies two eddy current loops, one with k =1 and τ = 70 μsec., and another with k = .36 and τ = 500 μsec. These estimates do not take into account the iron, which raises the DC inductance from 39 to 48 mH.

Measurements of the real and imaginary components of the magnet impedance are presented in Figures 4 and 5. Notation used is the same as that of eqn[24]. Measurements were made with excitation currents less than 1 amp in order that the measurements could be made on both warm and superconducting magnets, as well as magnets in various stages of assembly(7).

The measurement technique was specifically designed to be suitable for industrial environments where electrical interference and ground loops are present. The frequency range of 10 Hz to 3000Hz was selected for these measurements, as these frequencies were important for the estimation of standing wave damping and ripple current propagation in the complete 774 magnet Energy Doubler system.

The inductance of the magnets is about 45 mH up to 100 Hz, at which point it begins falling, reaching a value of about 18 mH at 1000 Hz. Investigation of magnets in states of partial assembly shows that the dip in the 100 to 1000 Hz range is due to the stainless steel cryogenic system, while the behavior above 1 kHz is due to the laminated collars and the bore tube.

A specific equivalent circuit to fit the inductance measurement is shown in Figure 6. The equivalent circuit is comprised of two nested eddy current loops. The inner loop has parameters k = .58 and τ = 650 μ sec., and the outer, k = 1.0 and τ = 64 μ sec. It is apparent that the presence of the iron yoke has substantially increased the coupling between the coil and the cryostat.

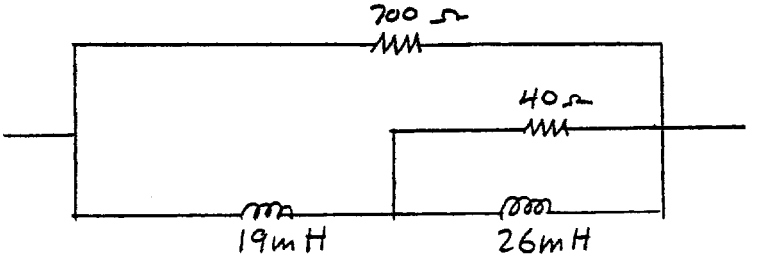

Figure 6. Equivalent Circuit for Fermilab Magnets

The solid lines in Figures 4 and 5 are based on the model. It

should be emphasized that the determination of the parameters is based entirely on the inductance measurements, and that the agreement with the data in Figure 4 is due to the constraints of the dispersion relations implicit in the model.

The roughly constant 2.5 mH difference between the warm and cold inductance measurements is believed to be due to the screening currents on the surfaces of the superconductor (equivalent to eddy currents with an infinite time constant, hence no power dissipation) excluding the interior volume of the superconductor from storing magnetic energy. The measurement implies a coupling constant k of about .05, leading to an estimate of 2.5% of the magnetic volume being inside the superconductor. This agrees with direct calculation of the B*H*dV integral over the volume of the superconductor. The interpretation of the coupling constant as representing magnetic volume is reviewed in section 3.

The real part of the impedance shows the quadratic frequency dependence up to about 100 Hz, and a somewhat lower frequency dependence at higher frequencies. Specifically, the AC resistance below 100 Hz is approximately:

$$R(\omega) \simeq \alpha \omega^2 = 2.0 \times 10^{-5} \omega^2 \qquad [71]$$

The power dissipated during a ramp at constant dI/dt is, as per eqns [52]+[64]:

$$P(t) = \alpha \left(\frac{dI_1}{dt}\right)^2 = 2.0 \times 10^{-5} \left(\frac{dI_1}{dt}\right)^2 \qquad [72]$$

This corresponds to 3.2 watts at 400 amps/sec. This is approximately the lowest non-hysteretic power loss seen in the Fermilab magnets(8). Magnets with much higher conductor braid eddy currents have been measured using the above technique, but the data did not show any difference. This in retrospect was to be expected based on the values in the model describing the effect seen at Brookhaven. It is now apparent that these effects can be seen as current or voltage transients at the magnet terminals as per eqns [55] and [61].

8. Conclusion

In summary, it is apparent that eddy current losses in magnets can be represented by simple equivalent circuits for the magnet impedance, and that the model can be useful in understanding how eddy currents can induce transients both in the magnet and in the power supply. It is also shown that there is a close relation between the AC power losses, the frequency dependence of the inductance, and transients in the magnetic fields, and that knowledge of one of these is often sufficient to predict the other two.

References

1. H. W. Bode, "Network Analysis and Feedback Amplifier Design", Van Norstrand (1945). See especially chapter 14 and the table on page 335.
2. E. A. Guillemin, "Theory of Linear Physical Systems", John Wiley & Sons (1963). See chapter 18 on Hilbert transforms.
3. J. P. Blewett, Proc. 1968 Summer Study on Superconducting Devices and Accelerators, Brookhaven Pub BNL 50155 (1969). The inductance equation is derived from stored energy relations in the above report.
4. C. H. Holbrow, Brookhaven ISABELLE Technical Memo No. 142, (8/14/79)
5. G. H. Morgan, J. Appl. Phys. 44(7), 3319 (1973).
6. A. V. Tollestrup, IEEE Trans MAG 15, 647 (1979)
7. The measurements are discussed in more detail in Fermilab internal report UPC 31, 1/79, by R. Shafer.
8. M. Wake, D. Gross, R. Yamada, and D. Blatchley, IEEE Trans MAG 15, 141 (1979).